The Canadian Mineralogist
Vol. 39, pp. 1377-1382 (2001)

THE CRYSTAL STRUCTURE OF PAARITE, THE NEWLY DISCOVERED 56 Å DERIVATIVE OF THE BISMUTHINITE–AIKINITE SOLID-SOLUTION SERIES

EMIL MAKOVICKY[§], DAN TOPA[¶] AND TONČI BALIĆ-ŽUNIĆ

Geological Institute, University of Copenhagen, Øster Voldgade 10, DK-1350 Copenhagen K, Denmark

ABSTRACT

We have determined the crystal structure of paarite, a newly discovered 56 Å derivative of the bismuthinite–aikinite series from the metamorphosed scheelite deposit of Felbertal, Austria. Its electron-microprobe-established composition is $Cu_{1.7}Pb_{1.7}Bi_{6.3}S_{12}$, and the structure-derived composition is $Cu_{1.6}Pb_{1.6}Bi_{6.4}S_{12}$, with *a* 4.007(1), *b* 55.998(8), *c* 11.512(2) Å, space group *Pmcn*, *Z* = 5. The structure has been solved by direct methods and difference-Fourier syntheses, and refined to a residual value R_1 of ~7.0%. The unit cell of this "fivefold derivative" contains two "bismuthinite-like" Bi_4S_6 ribbons and eight "krupkaite-like" $CuPbBi_3S_6$ ribbons. The fully occupied Cu sites occur in zigzag [001] rows at *y* = 0.15, 0.30, 0.70 and 0.85, comprising gladite-like and krupkaite-like intervals in the structure in regular 1:1 alternation. Coordination polyhedra have been analyzed using the polyhedron-distortion parameters devised recently by Balić-Žunić & Makovicky, and comparisons to the structures of salzburgite and lindströmite are given. This new derivative occurs at Felbertal both as independent grains and as a component of exsolution pairs with krupkaite.

Keywords: paarite, $Cu_{1.7}Pb_{1.7}Bi_{6.3}S_{12}$, bismuthinite–aikinite derivative, crystal structure, sulfosalt, Felbertal, scheelite deposit, Austria.

SOMMAIRE

Nous avons déterminé la structure cristalline de la paarite, dérivé à périodicité de 56 Å nouvellement découvert de la série bismuthinite–aikinite, provenant du gisement métamorphisé de scheelite de Felbertal, en Autriche. Sa composition, telle qu'établie avec une microsonde électronique, est $Cu_{1.7}Pb_{1.7}Bi_{6.3}S_{12}$, tandis que du point de vue structural, sa composition serait $Cu_{1.6}Pb_{1.6}Bi_{6.4}S_{12}$, avec *a* 4.007(1), *b* 55.998(8), *c* 11.512(2) Å, groupe spatial *Pmcn*, *Z* = 5. Nous avons résolu la structure par méthodes directes et par synthèses de Fourier par différence, et l'affinement s'est fait jusqu'à un résidu R_1 d'environ 7.0%. La maille élémentaire de ce dérivé à multiple de cinq contient deux rubans semblables à la bismuthinite, Bi_4S_6, et huit rubans de type krupkaïte, $CuPbBi_3S_6$. Les sites Cu, tous occupés, sont distribués en zigzag le long de [001] à *y* = 0.15, 0.30, 0.70 et 0.85, définissant ainsi des intervalles ressemblant à la gladite et à la krupkaïte dans la structure en alternance régulière 1:1. Les polyèdres autour des cations ont été analysés pour en évaluer la distorsion selon les paramètres récemment définis par Balić-Žunić et Makovicky, et nous comparons la structure à celles de la salzburgite et de la lindströmite. Ce dérivé a été découvert récemment à Felbertal sous forme de grains individuels et de lamelles d'exsolution, en coexistence avec la krupkaïte.

(Traduit par la Rédaction)

Mots-clés: paarite, $Cu_{1.7}Pb_{1.7}Bi_{6.3}S_{12}$, dérivé de la série bismuthinite–aikinite, structure cristalline, sulfosel, Felbertal, gisement de scheelite, Autriche.

INTRODUCTION

The sulfosalt material from the metamorphosed scheelite deposit of Felbertal, Austria (Thalhammer *et al.* 1989) has recently yielded a new mineral with a fourfold ordered superstructure of the bismuthinite–aikinite solid-solution series (Topa *et al.* 2000), approved by the IMA under the name of salzburgite. Now, another new derivative has been discovered, a fivefold ordered superstructure, chemically very close to salzburgite, yet clearly distinct from it.

Using the percentage of the aikinite end-member in the compounds of the aikinite $CuPbBiS_3$ (n_{aik} = 100) – bismuthinite Bi_2S_3 (n_{aik} = 0) solid-solution series as the best means of characterization (Makovicky & Makovicky 1978), the electron-microprobe-based estimates of composition of the current compound correspond to n_{aik} = 42, whereas those for the previously described, fourfold

---

[§] *E-mail address*: emilm@geo.geol.ku.dk

[¶] On leave from the Mineralogical Institute, University of Salzburg, Austria.

superstructure of salzburgite, to $n_{aik} = 40$ (Topa *et al.* 2000). The title compound occurs both as independent grains and as exsolution pairs with microprobe-estimated compositions of the two components equal to $n_{aik}(42)$ and $n_{aik}(47–48)$, respectively. These exsolution pairs are commonly further replaced by the pairs $n_{aik}(40)$ – $n_{aik}(48)$ and, finally, by the most common pair $n_{aik}(37)$ – $n_{aik}(48)$ (Topa *et al.*, in press). In the present report, we describe the fivefold superstructure; a mineralogical description of this phase, recently accepted by CNMMN IMA as a new mineral species, *paarite*, will follow. We should stress that this compound is very different from lindströmite, the other fivefold superstructure in the series, with ideal $n_{aik} = 60$, described by Horiuchi & Wuensch (1977).

EXPERIMENTAL

The chemical composition of the crystal was obtained by electron-microprobe analysis before its extraction from a polished section. We used a JEOL–8600 electron microprobe equipped with Link EXL software with on-line ZAF correction. Analytical conditions employed were 25 kV and 30 nA; synthetic and natural sulfide standards were used. The averaged analytical results (wt.%) for five points on the crystal fragment that was subsequently used for crystal-structure analysis are: Cu 4.79(3), Fe 0.08(1), Pb 16.7(1), Bi 60.8(2), S 17.83(4), total 100.20 wt.%. The resulting empirical formula is $Cu_{1.62}Fe_{0.03}Pb_{1.74}Bi_{6.29}S_{11.99}$. It becomes $Cu_{1.66}Pb_{1.71}Bi_{6.32}S_{11.99}$ with the $Fe^{2+} \longrightarrow Cu^{+}$ conversion compensated for by the appropriate $Pb^{2+} \longrightarrow Bi^{3+}$ conversion, *i.e.*, $n_{aik} = 42.1$ or, alternatively, the mol.% of the krupkaite end-member is equal to 84.2% and that of the bismuthinite end-member is 15.8%. The observed range of n_{aik} values, Δn_{aik}, is equal to 0.7.

TABLE 1. CRYSTAL DATA AND STRUCTURE-REFINEMENT INFORMATION FOR PAARITE, THE 56 Å DERIVATIVE OF THE BISMUTHINITE–AIKINITE SOLID-SOLUTION SERIES

Measured reflections:	15242
Unique reflections:	3050 (2913 with $I > 2\sigma_I$)
Temperature:	298 K
Space group:	*Pmcn*
Unit-cell parameters:	
a	4.0070(6) Å
b	55.998(8) Å
c	11.512(2) Å
V (refined from reflections with $I>10\sigma_I$)	2583(1) Å^3
Z	5
ϱ_c	6.944 g/cm^3
μ	70.126 mm^{-1}
Full-matrix refinement	
Weighting scheme:	
$1/\{\sigma^2_{Fo}{}^2 + [0.0939(\mathrm{Max}(F_O{}^2,0) + 2F_C{}^2)/3]^2 + 51.399(\mathrm{Max}(F_O{}^2,0) + 2F_C{}^2)/3\}$ (giving a flat analysis of variance in terms of $F_C{}^2$)	
R factors:	
$wR_2 = \{\Sigma[w(F_O{}^2 - F_C{}^2)^2] / \Sigma[w(F_O{}^2)^2]\}^{1/2} = 0.1962$	
$R_1 = \Sigma w \| F_C\| - \|F_O\|\| / \Sigma w\|F_O\| = 0.0703$ (for $F_O > 4\sigma_{Fo}$), 0.0988 (all)	
$R_\sigma = \Sigma\sigma_{Fo}{}^2 / \Sigma F_o{}^2 = 0.0517$	
$R_{INT} = \Sigma\|F_O{}^2 - \langle F_O{}^2\rangle\| / \Sigma F_O{}^2$ (for symmetry equivalents) = 0.0899	
GooF:	1.122
Scale factor:	0.02167

A crystal fragment with an irregular shape and 0.04–0.09 mm in diameter was measured on a Bruker AXS four-circle diffractometer equipped with CCD 1000K area detector (6.25 cm × 6.25 cm active detection-area, 512 × 512 pixels) and a flat graphite monochromator using Mo*K*α radiation from a fine-focus sealed X-ray tube. The sample – detector distance was fixed at 6 cm. In all, 2080 static exposures 0.25° apart were made, each measurement taking 45 s, with 94.5% coverage and average redundancy of 5.8 inside the limits of the angular span covered. The maximum 2θ value covered was 54°, and Miller index limits were $5 \le h \le 4$, $69 \le k \le 69$, $14 \le l \le 14$. The SMART system of programs was used for unit-cell determination and data collection (Table 1), SAINT+ for the calculation of integrated intensities, and SHELXTL for the structure solution and refinement (all Bruker AXS products). For the empirical absorption-correction, based on reflection measurements at different azimuthal angles and measurements of equivalent reflections, program XPREP from the SHELXTL package was used, and yielded a merging R_{INT} factor of 0.0899 compared to 0.2050 before absorption correction. Minimum and maximum transmission factors were 0.0006 and 0.0127, respectively. This indicates a pronounced anisotropy of crystal outlines, causing the elevated R values (Table 1). However, no other grains of paarite suitable for crystallographic analysis were found, and we had to use the present crystal fragment. The systematic absences (*h*0*l*, $l = 2n + 1$, and *hk*0 for $h + k = 2n + 1$) are consistent with space groups $P2_1cn$ and *Pmcn*. The latter was chosen as consistent with structures of the bismuthinite – aikinite family. Solution of the structure by direct methods revealed the positions of Bi and Pb atoms and of all S atoms. In subsequent refinements, the positions of the Cu atoms were deduced from the difference-Fourier syntheses.

After the final refinement with anisotropic displacement-factors used for all the atoms, the highest residual peak was 3 e/Å^3, 0.86 Å from Bi3, and the deepest hole, –3 e/Å^3, 1.64Å from S 11. The refinement was stopped when the maximum shift/e.s.d. for varied parameters dropped below 1. The results of the refinement are represented in Table 2 and Figure 1, with interatomic distances in Table 3 (deposited). Structure factors may be obtained from the Depository of Unpublished Data, CISTI, National Research Council, Ottawa, Ontario K1A 0S2, Canada.

Description of the structure

The present structure contains 10 *en échelon* Me_4S_6 ribbons in the unit cell, arranged in two parallel rows. Eight of them are "krupkaite-like ribbons" $CuPbBi_3S_6$ (Mumme *et al.* 1976), two are "bismuthinite-like ribbons" Bi_4S_6 (Fig. 1). The latter ribbons are as far apart

TABLE 2. POSITIONAL AND DISPLACEMENT PARAMETERS FOR PAARITE, THE 56 Å DERIVATIVE OF THE BISMUTHINITE–AIKINITE SOLID-SOLUTION SERIES

Atom	x	y	z	U_{11}	U_{22}	U_{33}	U_{23}	Ueq
Bi1	0.75	0.06455(2)	0.5074(1)	0.0398(8)	0.0420(7)	0.0437(9)	0.0039(6)	0.0418(4)
Bi2	0.25	0.00787(2)	0.6575(1)	0.0434(8)	0.0447(7)	0.0433(9)	0.0017(6)	0.0438(4)
Bi3	0.75	0.03372(2)	0.0209(1)	0.0393(8)	0.0395(7)	0.0428(9)	0.0022(6)	0.0405(4)
Bi4	0.25	0.16240(2)	-0.0290(1)	0.0410(8)	0.0468(8)	0.0404(8)	0.0013(6)	0.0427(4)
Bi5	0.25	0.09265(3)	0.1476(2)	0.0454(8)	0.0432(7)	0.0462(9)	-0.0031(6)	0.0449(4)
Bi6	0.75	0.23416(2)	0.0081(1)	0.0397(8)	0.0435(7)	0.0426(9)	0.0045(6)	0.0419(4)
Bi7	0.25	0.13711(3)	0.4743(1)	0.0403(8)	0.0473(7)	0.0393(8)	0.0027(6)	0.0423(4)
Bi8	0.25	0.29219(3)	0.1460(1)	0.0451(8)	0.0477(8)	0.0413(8)	-0.0045(6)	0.0447(4)
Pb1	0.75	0.09871(3)	0.8171(2)	0.0503(9)	0.0493(8)	0.0470(9)	0.0046(7)	0.0489(4)
Pb2	0.75	0.19974(3)	0.3167(2)	0.0484(9)	0.0496(8)	0.0470(9)	0.0057(9)	0.0483(4)
Cu1	0.75	0.15692(9)	0.7192(5)	0.050(3)	0.055(3)	0.041(3)	0.000(2)	0.048(1)
Cu2	0.75	0.14191(9)	0.2197(5)	0.052(3)	0.052(3)	0.044(3)	0.004(2)	0.050(1)
S1	0.25	0.0892(2)	0.6086(9)	0.049(5)	0.036(4)	0.036(5)	0.000(4)	0.040(2)
S2	0.25	0.0252(2)	0.4484(8)	0.040(5)	0.044(4)	0.034(5)	-0.003(4)	0.039(2)
S3	0.75	0.0402(2)	0.7084(9)	0.039(5)	0.031(4)	0.043(5)	0.005(4)	0.038(2)
S4	0.25	0.0104(2)	0.1270(9)	0.039(5)	0.049(5)	0.034(5)	0.004(4)	0.041(2)
S5	0.25	0.0714(2)	0.9480(9)	0.035(5)	0.046(5)	0.033(5)	0.004(4)	0.038(2)
S6	0.25	0.1379(2)	0.7723(9)	0.043(5)	0.033(4)	0.042(5)	-0.001(4)	0.039(2)
S7	0.75	0.1881(2)	0.8673(9)	0.046(5)	0.032(4)	0.042(5)	-0.001(4)	0.040(2)
S8	0.75	0.1252(2)	0.0362(9)	0.042(5)	0.049(5)	0.036(5)	0.003(4)	0.043(2)
S9	0.75	0.0613(2)	0.2126(9)	0.041(5)	0.036(4)	0.039(5)	0.005(4)	0.039(2)
S10	0.25	0.2103(1)	0.1101(9)	0.043(5)	0.028(4)	0.045(5)	0.004(4)	0.039(2)
S11	0.25	0.2281(1)	0.4437(9)	0.045(5)	0.029(4)	0.044(5)	0.002(4)	0.040(2)
S12	0.25	0.1609(2)	0.2748(9)	0.040(5)	0.043(5)	0.034(5)	-0.001(4)	0.039(2)
S13	0.75	0.1120(2)	0.3727(9)	0.044(5)	0.035(4)	0.037(5)	-0.007(4)	0.039(2)
S14	0.75	0.1751(2)	0.5372(9)	0.045(5)	0.038(4)	0.039(5)	-0.001(4)	0.041(2)
S15	0.75	0.2394(2)	0.7058(8)	0.041(5)	0.039(4)	0.037(5)	-0.008(4)	0.039(2)

as possible, at $y = 0.0$ and 0.5, respectively, and related by c-glide operators.

The tetrahedrally coordinated copper atoms flanking unilaterally the "krupkaite-like ribbons" are arranged in zig-zag [001] rows positioned at $y \approx 0.15$, 0.30, 0.70 and 0.85. They display full site-occupancy. The intermediate rows of tetrahedra appear unoccupied; no additional Cu atoms were found in these positions, and the structure thus seems to be fully ordered. The intervals between the copper [001] rows respectively correspond to those observed in gladite and krupkaite (Synečeк & Hybler 1974, Kohatsu & Wuensch 1976) in regular alternation and in a 1:1 ratio.

The fully occupied Cu1 and Cu2 sites have a slightly eccentric tetrahedral coordination, typical for all aikinite–bismuthinite derivatives (*e.g.*, Kohatsu & Wuensch 1976). Adjacent to these are monocapped trigonal coordination prisms of lead, Pb1 and Pb2 (Fig. 2). All the remaining large-cation positions are fully occupied by Bi atoms.

The microprobe-derived composition of the paarite crystal under study, $Cu_{1.7}Pb_{1.7}Bi_{6.3}S_{12}$, is slightly richer in Cu and Bi than indicated by the idealized formula derived from the refined crystal structure. The difference of about 0.1 Cu per subcell formula unit is distributed over the empty tetrahedral sites without a statistically significant accumulation at a particular site.

The ideal formula of the present phase based on the crystal-structure analysis is $Cu_{1.6}Pb_{1.6}Bi_{6.4}S_{12}$, *i.e.*, 4.72 wt.% Cu, 15.38% Pb, 62.05% Bi and 17.85% S. It leads to a theoretical n_{aik} of 40, *i.e.*, 80 mol.% of the krupkaite end-member and 20 mol.% of the bismuthinite end-member.

Relations to lindströmite

The only known fivefold superstructure of the bismuthinite–aikinite series until now, lindströmite $Cu_3Pb_3Bi_7S_{15}$ (Horiuchi & Wuensch 1977), has an ideal n_{aik} of 60. It contains eight krupkaite-like ribbons $CuPbBi_3S_6$ and two aikinite-like ribbons $Cu_2Pb_2Bi_2S_6$ in the unit cell (Fig. 3). In this way, it is a mirror image of the current structure, in which the latter two ribbons are replaced by bismuthinite-like ribbons Bi_4S_6. The space group is the same, *Pmcn*, in the present orientation. However, in lindströmite the Cu-free and Cu-occupied ends of krupkaite ribbons are interchanged in relation to those in the current phase. This results in an interchange of Cu-occupied and Cu-free (010) planes of coordination tetrahedra between these two structures and in an entirely different type of intervals between the Cu-occupied (010) planes: the regular alternation of single gladite-like and krupkaite-like intervals in our phase is replaced by a regular alternation of two krupkaite-like intervals with a single, ½*b*-subcell-wide aikinite-like interval.

Coordination polyhedra

The present structure contains eight atoms of bismuth and two atoms of lead. Bi 1, 3, 4, 6, 7 constitute the apical Bi polyhedra of Me_4S_6 ribbons denoted as A2 by Berlepsch *et al*. (2001), whereas Bi 2, 5, 8 and Pb 1, 2 occupy the "central" polyhedra of these ribbons, denoted as Z2 by Berlepsch *et al*. (2001) (Fig. 1).

In order to study the differences in coordination of these three groups, a coordination analysis similar to that in Topa *et al.* (2000) will be undertaken, somewhat different from the usual examination of interatomic distances in Table 3. Following the principles given in

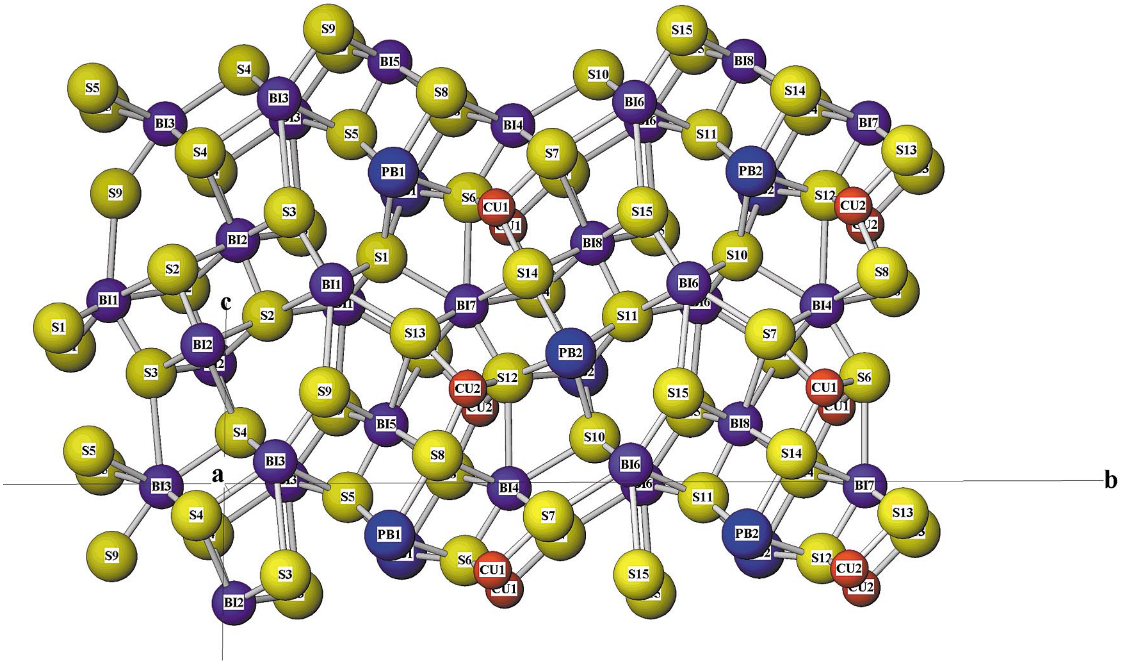

FIG. 1. Labeled atoms in the crystal structure of paarite, $Cu_{1.7}Pb_{1.7}Bi_{6.3}S_{12}$ (an aikinite–bismuthinite derivative with n_{aik} = 42). Projection on (100), directions of crystal axes are indicated.

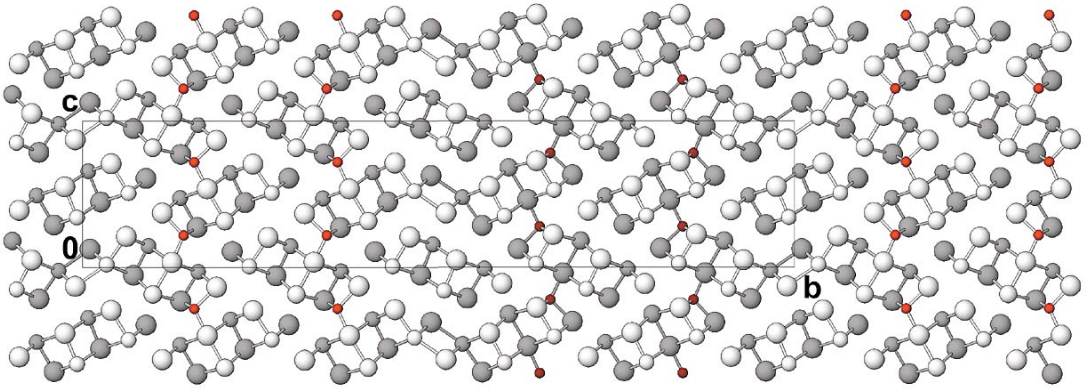

FIG. 2. The crystal structure of $Cu_{1.7}Pb_{1.7}B_{6.3}S_{12}$. In the order of decreasing size, the circles indicate S, Pb, Bi and Cu (red). The krupkaite-like intervals (narrower) and gladite-like intervals (broader) between Cu-occupied planes (010) are prominent. Void and shaded circles indicate atoms at two *x* levels 2 Å apart.

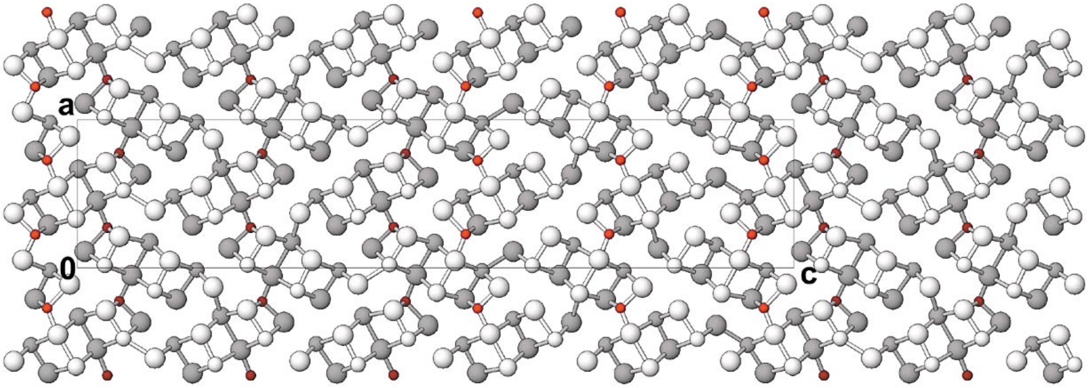

FIG. 3. The crystal structure of $Cu_3Pb_3Bi_7S_{15}$ (lindströmite; Horiuchi & Wuensch 1977). Graphic conventions as in Figure 2. The krupkaite-like intervals (broader) and the aikinite-like intervals (narrower) between Cu-occupied (010) planes (red) are prominent.

TABLE 4. POLYHEDRON DISTORTION PARAMETERS FOR CATIONS IN PAARITE, THE 56 Å DERIVATIVE OF THE BISMUTHINITE–AIKINITE SOLID-SOLUTION SERIES

Atom	CN	Sphere radius, ligand scatter[(1)]	Sphere volume	Polyhedron volume	Volume[(2)] distortion	Eccen-tricity[(3)]	Spher-icity[(4)]
Bi1	7	2.957 ± 0.031	108.313	36.951	0.0985	0.3668	0.9684
Bi2	7	2.982 ± 0.039	111.022	36.731	0.1257	0.4138	0.9608
Bi3	7	2.959 ± 0.108	108.471	36.749	0.1047	0.4211	0.8905
Bi4	7	2.966 ± 0.065	109.298	37.274	0.0988	0.3814	0.9342
Bi5	7	3.015 ± 0.061	114.821	37.819	0.1296	0.4557	0.9389
Bi6	7	2.946 ± 0.077	107.086	36.435	0.1009	0.3853	0.9213
Bi7	7	2.952 ± 0.042	107.758	36.857	0.0963	0.3738	0.9578
Bi8	7	3.003 ± 0.059	113.401	37.46	0.1271	0.4443	0.9408
Pb1	7	3.030 ± 0.028	116.564	38.315	0.1314	0.1525	0.9727
Pb2	7	3.023 ± 0.019	115.706	38.242	0.1266	0.1598	0.9809
Cu1	4	2.36	55.057	6.599	0.0217	0.0981	1
Cu2	4	2.356	54.751	6.524	0.0274	0.0964	1

The centroid parameters used are defined in Balić-Žunić & Makovicky (1996) and Makovicky & Balić-Žunić (1998). The volume distortions are calculated using the maximum volume polyhedra for respective CN (7 = regular pentagonal bipyramid, 4 = regular tetrahedron) as ideal reference.

(1) Ligand scatter about the least-squares-fitted circumscribed sphere is calculated as a standard deviation of ligand positions in respect to this sphere. It is not identical with the uncertainty in the value of the sphere radius or in the calculated volumes, caused by standard errors of the atom positions.

(2) Volume distortion $\upsilon = [V(\text{ideal}) - V(\text{polyhedron})] / V(\text{ideal})$ to be multiplied by 100 to obtain percentage.

(3) "Volume-based" eccentricity $ECC_V = 1 - [(r_s - \Delta)/r_s]^3$, where r_s is the radius of the circumscribed sphere, and Δ is the distance between the sphere's center ("centroid") and the central atom.

(4) "Volume-based" sphericity $SPH_V = 1 - 3\sigma_r/r_s$, where σ_r is a standard deviation of ligand positions about the radius r_s.

Balić-Žunić & Makovicky (1996) and Makovicky & Balić-Žunić (1998), and used by Berlepsch *et al.* (2001) for all meneghinite homologues, including the hitherto published structures of the aikinite–bismuthinite series, a least-squares-fitted sphere is circumscribed to the coordination polyhedron. A coordination number (CN) of 7 is used for all Bi and Pb sites, whereas CN = 4 for the copper sites, in agreement with a number of previous publications on the bismuthinite–aikinite group.

The volume of the circumscribed sphere (Table 4) is compared to that of the coordination polyhedron and to the volume of an ideal polyhedron inscribed in the same sphere; this approach yields a measure of polyhedron distortion (Table 4). "Sphericity" is a measure of the fit of ligands to the sphere, and "eccentricity" expresses a displacement of the cation from the center of the sphere. The relevant definitions are given in the footnote to Table 4.

The central Z2 cations of the Me_4S_6 ribbons have distinctly larger sphere volumes than the apical A2 cations, although the polyhedron volumes do not invariably follow suit (Table 4). Polyhedron and sphere volumes for Pb are marginally larger than those of corresponding Bi atoms. Volume distortion is distinctly greater for the central cation polyhedra, both for Pb and Bi. All these findings agree with the conclusions reached by Berlepsch *et al.* (2001) for the entire bismuthinite–aikinite series, but they are here obtained at a higher level of accuracy. "Central" Bi5 and Bi8 have a distinctly higher eccentricity; that of Bi2 is lower, at the upper limits of eccentricity for "apical" Bi sites (Table 4). The eccentricity of Pb, however, is much lower; lead has a marginally better sphericity than all Bi sites, which all show rather uniform characteristics.

Comparison with the data for salzburgite, with the composition estimated by electron-microprobe analyses to be $Cu_{1.6}Pb_{1.6}Bi_{6.4}S_{12}$ (Table 4 in Topa *et al.* 2000), shows a near-identity of all these features between the two chemically close compounds. Thus, all the conclusions reached for salzburgite can be transferred to the present structure. This holds also for the fully occupied copper sites in these two structures (Table 4 in the present work and Table 4 in Topa *et al.* 2000), slightly eccentric in a way typical of the structures of the bismuthinite–aikinite series (Fig. 1). The increased unit-cell (subcell) volume as a function of proportion of Bi_2S_3 is clearly distributed over the individual cation polyhedra: the Bi–S polyhedra in the present compound and salzburgite have polyhedron volumes of 36.4–37.8 $Å^3$, whereas those in the end-member Bi_2S_3 are only in the range 35.5–35.9 $Å^3$ (Kupčík & Veselá-Nováková 1970).

With respect to the occupancy of tetrahedral sites by copper, paarite is close to an ideal structural model with respectively fully occupied and empty tetrahedral sites. In this, it contrasts with salzburgite in which, besides fully occupied Cu sites, a site with 71% occupancy and two sites with 10% occupancy also were detected.

ACKNOWLEDGEMENTS

This research was supported by the research and equipment grants from the National Research Council of Denmark (Natural Sciences). Active interest and support of Prof. W. Paar (Salzburg) and of the geological departments of the University of Copenhagen and the University of Salzburg, as well as the professional assistance of Mrs. Britta Munch and Mrs. Camilla Sarantaris, are gratefully acknowledged. Valuable comments of Drs. P. Berlepsch, A. Pring and R.F. Martin helped to improve the manuscript.

REFERENCES

BALIĆ-ŽUNIĆ, T. & MAKOVICKY, E. (1996): Determination of the centroid or 'the best centre' of a coordination polyhedron. *Acta Crystallogr.* **B52**, 78-81.

BERLEPSCH, P., MAKOVICKY, E. & BALIĆ-ŽUNIĆ, T. (2001): The crystal chemistry of meneghinite homologues and related compounds. *Neues Jahrb. Mineral., Monatsh.*, 115-135.

HORIUCHI, H. & WUENSCH, B.J. (1977): Lindströmite, $Cu_3Pb_3Bi_7S_{15}$; its space group and ordering scheme for metal atoms in the crystal structure. *Can. Mineral.* **15**, 527-535.

KOHATSU, I. & WUENSCH, B.J. (1976): The crystal structure of gladite, $PbCuBi_5S_9$, a superstructure intermediate in the series Bi_2S_3–$PbCuBiS_3$. *Acta Crystallogr.* **B32**, 2401-2409.

KUPČÍK, V. & VESELÁ-NOVÁKOVÁ, L. (1970): Zur Kristallstruktur des Bismuthinits, Bi_2S_3. *Tschermaks Mineral. Petrogr. Mitt.* **14**, 55-59.

MAKOVICKY, E. & BALIĆ-ŽUNIĆ, T. (1998): New measure of distortion for coordination polyhedra. *Acta Crystallogr.* **B54**, 766-773.

________ & MAKOVICKY, M. (1978): Representation of compositions in the bismuthinite–aikinite series. *Can. Mineral.* **16**, 405-409.

MUMME, W.G., WELIN, E. & WUENSCH, B.J. (1976): Crystal chemistry and proposed nomenclature for sulfosalts intermediate in the system bismuthinite–aikinite (Bi_2S_3–$CuPbBiS_3$). *Am. Mineral.* **61**, 15-20.

SYNEČEK, V. & HYBLER, J. (1974): The crystal structures of krupkaite, $CuPbBi_3S_6$, and of gladite, $CuPbBi_5S_9$, and the classification of superstructures in the bismuthinite–aikinite group. *Neues Jahrb. Mineral., Monatsh.*, 541-560.

THALHAMMER, O.A.R., STUMPFL, E.F. & JAHODA, R. (1989): The Mittersill scheelite deposit, Austria. *Econ. Geol.* **84**, 1153-1171.

TOPA, D., BALIĆ-ŽUNIĆ, T. & MAKOVICKY, E. (2000): The crystal structure of $Cu_{1.6}Pb_{1.6}Bi_{6.4}S_{12}$, a new 44.8 Å derivative of the bismuthinite–aikinite solid-solution series. *Can. Mineral.* **38**, 611-616.

________, MAKOVICKY, E. & PAAR, W. (2002): Composition ranges and exsolution pairs for the members of the bismuthinite–aikinite series from Felbertal, Austria. *Can. Mineral.* **40** (in press).

Received February 8, 2001, revised manuscript accepted August 31, 2001.